

2

AEROSPACE REPORT NO.
ATR-92(8476)-1

AD-A258 464



Exact Calculation of Light Scattering from a Particle on a Mirror

Prepared by

B. R. JOHNSON
Space and Environment Technology Center
Technology Operations

DTIC
ELECTE
DEC 29 1992
S A D

15 November 1992

Prepared for
VICE PRESIDENT
Technology Operations

This document has been approved
for public release and sale; its
distribution is unlimited.

Engineering and Technology Group

THE AEROSPACE CORPORATION
El Segundo, California

PUBLIC DISTRIBUTION IS AUTHORIZED

92 12 28 031

425689
92-32856

TECHNOLOGY OPERATIONS

The Aerospace Corporation functions as an "architect-engineer" for national security programs, specializing in advanced military space systems. The Corporation's Technology Operations supports the effective and timely development and operation of national security systems through scientific research and the application of advanced technology. Vital to the success of the Corporation is the technical staff's wide-ranging expertise and its ability to stay abreast of new technological developments and program support issues associated with rapidly evolving space systems. Contributing capabilities are provided by these individual Technology Centers:

Electronics Technology Center: Microelectronics, solid-state device physics, VLSI reliability, compound semiconductors, radiation hardening, data storage technologies, infrared detector devices and testing; electro-optics, quantum electronics, solid-state lasers, optical propagation and communications; cw and pulsed chemical laser development, optical resonators, beam control, atmospheric propagation, and laser effects and countermeasures; atomic frequency standards, applied laser spectroscopy, laser chemistry, laser optoelectronics, phase conjugation and coherent imaging, solar cell physics, battery electrochemistry, battery testing and evaluation.

Mechanics and Materials Technology Center: Evaluation and characterization of new materials: metals, alloys, ceramics, polymers and their composites, and new forms of carbon; development and analysis of thin films and deposition techniques; nondestructive evaluation, component failure analysis and reliability; fracture mechanics and stress corrosion; development and evaluation of hardened components; analysis and evaluation of materials at cryogenic and elevated temperatures; launch vehicle and reentry fluid mechanics, heat transfer and flight dynamics; chemical and electric propulsion; spacecraft structural mechanics, spacecraft survivability and vulnerability assessment; contamination, thermal and structural control; high temperature thermomechanics, gas kinetics and radiation; lubrication and surface phenomena.

Space and Environment Technology Center: Magnetospheric, auroral and cosmic ray physics, wave-particle interactions, magnetospheric plasma waves; atmospheric and ionospheric physics, density and composition of the upper atmosphere, remote sensing using atmospheric radiation; solar physics, infrared astronomy, infrared signature analysis; effects of solar activity, magnetic storms and nuclear explosions on the earth's atmosphere, ionosphere and magnetosphere; effects of electromagnetic and particulate radiations on space systems; space instrumentation; propellant chemistry, chemical dynamics, environmental chemistry, trace detection; atmospheric chemical reactions, atmospheric optics, light scattering, state-specific chemical reactions and radiative signatures of missile plumes, and sensor out-of-field-of-view rejection.

EXACT CALCULATION OF LIGHT SCATTERING FROM A PARTICLE ON A MIRROR

Prepared by

B. R. Johnson
Space and Environment Technology Center
Technology Operations

15 November 1992

Engineering and Technology Group
THE AEROSPACE CORPORATION
El Segundo, CA 90245-4691


Prepared for
VICE PRESIDENT
Technology Operations

Accession For	
NTIS CRA&I	<input checked="" type="checkbox"/>
DIC TAB	<input type="checkbox"/>
Unannounced	<input type="checkbox"/>
Justification	
By	
Distribution /	
Availability Codes	
Dist	Avail and for Special
A-1	


PUBLIC DISTRIBUTION IS AUTHORIZED

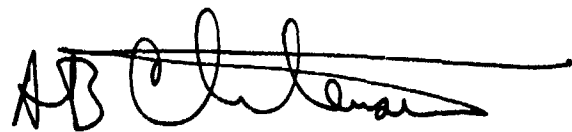
EXACT CALCULATION OF LIGHT SCATTERING FROM A PARTICLE ON A MIRROR

Prepared


B. R. Johnson
Target Signatures and Backgrounds
Department

Approved


C. J. Rice, Director
Target Signatures and Backgrounds
Department
Space and Environment Technology Center


A. B. Christensen, Principal Director
Space and Environment Technology Center
Technology Operations

ABSTRACT

Exact methods have been developed for calculating light scattering from particles on a perfectly reflecting surface. The computed solutions obey Maxwell's equations and the appropriate boundary conditions. A brief discussion of the theory is followed by a presentation and discussion of selected scattering results. Comparisons are made with the predictions of Young's forward scatter Mie theory model. Under certain conditions the exact results differ significantly from Mie theory. The exact differential cross sections exhibit large amplitude oscillations that are not predicted by Mie theory. The bidirectional reflectance distribution function (BRDF) is also calculated using exact scattering theory for both spherical and hemispherical particles that are both absorptive (complex index of refraction) and nonabsorptive (real index of refraction). These exact BRDF results are compared to the predictions of Young's model.

ACKNOWLEDGMENT

This work was supported by Aerospace sponsored research.

CONTENTS

1.	INTRODUCTION.....	1
2.	EXACT METHODS	3
2.1	Method of images.....	3
2.2	Spherical particles.....	4
2.3.	Nonspherical particles.....	4
2.4	Hemispherical particles.....	4
3.	FORWARD-SCATTER MIE APPROXIMATION.....	5
4.	RESULTS.....	7
4.1	Differential cross sections	7
4.2	BRDF	10
5.	CONCLUDING REMARKS.....	17
	REFERENCES.....	19

FIGURES

1. Illustration of the method of images	3
2. Geometry of Young's forward-scatter Mie theory model.....	5
3. Differential scattering cross section for particle on mirror.....	8
4. Differential scattering cross section vs particle diameter at fixed scattering angles, with $n = 1.8$, $\lambda = 10 \mu\text{m}$	9
5. Differential scattering cross section vs particle diameter at fixed scattering angles, with $n = 2.7 + 0.51j$, $\lambda = 10 \mu\text{m}$	11
6. Density-weighted differential scattering cross section vs particle diameter at fixed scattering angles	12
7. Upper particle diameter limit of BRDF integral that evaluates to 10, 25, 50, 75, and 90 percent of the final BRDF value.....	13
8. BRDF for cleanliness level 300 surface at $\lambda = 10 \mu\text{m}$	14
9. Comparison of BRDFs for transparent ($n = 1.8$) and absorptive ($n = 2.7 + 0.51j$) particles	15

1. INTRODUCTION

Light scattering from particle contaminants on the surfaces of mirrors is one of the main contributors to stray radiation in satellite-borne surveillance systems. This limits the ability of the system to detect and track dim targets that are near a bright radiation source such as the Earth. The designers of these systems need reliable methods for quantitatively estimating the intensity of the scattered light in order to minimize the effects of stray radiation.

Previous laboratory investigations of this problem include both experimental measurements and theoretical calculations.¹⁻³ The model systems in these studies were spherical particles on a conducting plane. The prior theoretical calculations have been based on approximation methods that neglect the interaction between the particle and the reflecting surface.

Recently, we have developed and implemented several exact procedures for calculating light scattering by spherical particles and also certain types of nonspherical particles on a perfectly conducting plane surface. It is the purpose of this report to present some selected results of these exact calculations and to also compare these results with the predictions of Young's forward-scatter Mie theory method.¹

2. EXACT METHODS

2.1 METHOD OF IMAGES

The scattering problem is illustrated in Fig 1a. A particle rests on a perfect reflecting (infinite conductivity) plane surface mirror. An electromagnetic plane wave, represented by the electric field vector E_{inc} , is incident upon this system. This gives rise to a reflected plane wave, E_{ref} , and a radially outgoing scattered wave, E_{scat} . In the region above the mirror, the field must satisfy Maxwell's field equations and also satisfy the condition that there can be no tangential component of the electric field at the reflecting surface. The problem, as presently formulated, is quite difficult to solve because of the boundary condition that must be satisfied at the surface. The method of images can be used to reformulate the problem in a much simpler form.

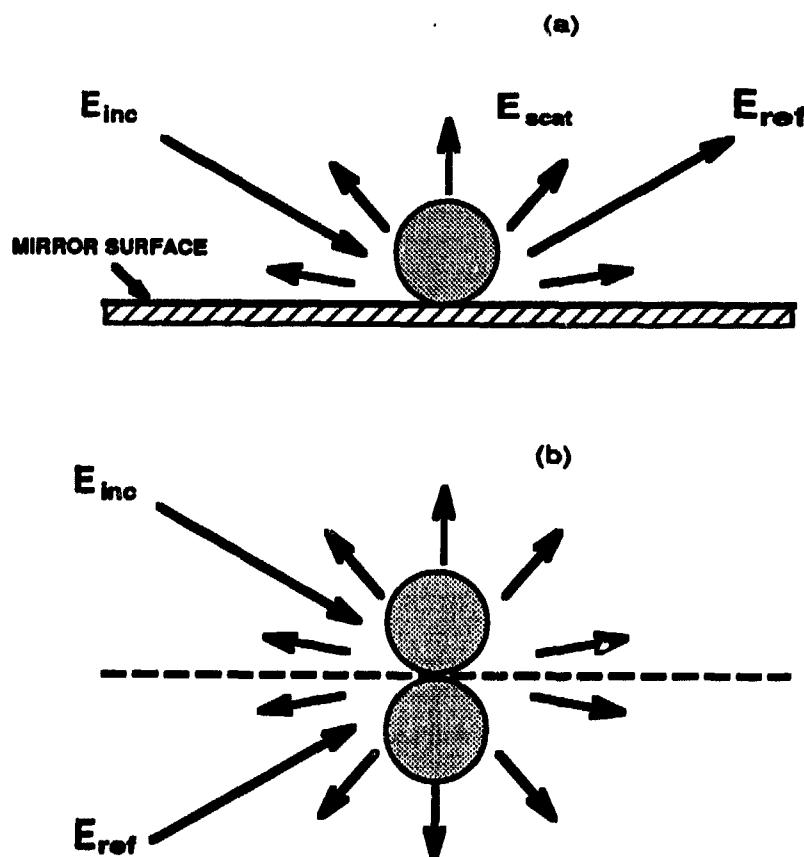


Figure 1. Illustration of the method of images: (a) physical system; (b) equivalent method-of-images system.

An observer looking down on the system in Fig 1a will see the particle, the mirror image of the particle, the source of the incident wave (e.g., a laser), and the mirror image of the source. The image of the source is the apparent origin of the reflected wave. This apparent picture is turned into reality by creating the system shown in Fig. 1b where the mirror has been removed, the image of the particle has been replaced by a real particle, and the image of the source has been replaced by a real source. The image source is the origin of the reflected wave, E_{ref} , which is shown in the figure as originating below the surface of the mirror and incident on the two-particle system along with the original incident wave, E_{inc} . It can be shown that the solution to the scattering problem shown in Fig 1b, in the region above the mirror, is identical to the solution to the problem shown in Fig. 1a in this same region. The system shown in Fig. 1b is easier to solve than the original system because no explicit surface boundary conditions are imposed on the solution. The boundary conditions at the surface of the mirror are automatically satisfied as a natural consequence of the symmetry of the system.

2.2 SPHERICAL PARTICLES

The problem is to calculate the scattering from the two-particle system shown in Fig. 1b. If the particles are spherical, the multipole expansion method of Bruning and Lo⁴ can be directly applied to this system. The fact that this system has two incident beams rather than a single incident beam (as is the original Bruning and Lo formulation) causes no difficulties. On the contrary, it actually simplifies the calculation by introducing symmetry to the problem. An efficient computer program has been developed to carry out these calculations. The complete details of this method and the computer program are given in ref. [5].

2.3. NONSPHERICAL PARTICLES

The illustrations in Figs. 1a and 1b show spherical particles. However, it is obvious that the method of images is valid for nonspherical particles as well. A numerical procedure, based on the invariant imbedding T-matrix method⁶ has been developed to calculate the scattering from the resulting two-particle system consisting of the nonspherical particle and its mirror image. At present, the computer program that implements these calculations is limited to particles with dimensions that do not exceed about three times the wavelength of the radiation. Because of this limitation, we did not use this method herein.

2.4 HEMISPHERICAL PARTICLES

The case of a hemispherically shaped particle is special. The particle and the image particle combine to form a single complete sphere. The resulting scattering problem can be solved easily and exactly by the application of Mie theory. The only difference between this problem and problems ordinarily encountered in Mie theory is the presence of two incident waves rather than a single incident wave. A Mie scattering program has been modified to handle this case.

3. FORWARD-SCATTER MIE APPROXIMATION

Young obtained good agreement between experiment and a simple theoretical model based on Mie theory. The geometry of this model is illustrated in Fig. 2. An incoming beam of light is scattered by the particle. The scattering process is assumed not to be affected by the presence of the mirror and is calculated using ordinary Mie theory. The light scattered by the particle can reach the detector by the two paths shown in the figure. The backscatter ray, which proceeds directly from the particle to the detector, is scattered through a large angle. Therefore, it is usually much weaker than the (reflected) forward-scatter ray and can be neglected. Thus, in this approximation, only the reflected forward-scatter ray contributes to the signal received by the detector. It is further assumed that the presence of the particle does not interfere with the propagation of the reflected forward-scatter ray from the mirror to the detector. Hence, the forward scatter Mie approximation is simply a Mie theory calculation with the scattering angle measured from the direction of the specularly reflected beam.

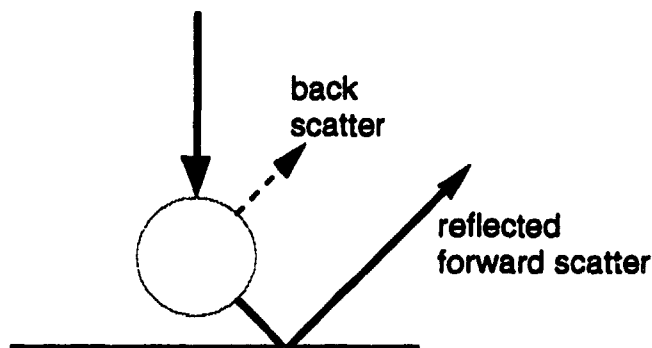


Figure 2. Geometry of Young's forward-scatter Mie theory model.

4. RESULTS

Results obtained by exact theory and Youngs forward-scatter Mie theory are presented and compared. The results are expressed as differential cross sections when the scattering is from a single particle on a reflecting surface and as bidirectional reflectance distribution functions (BRDF) when the scattering is from a distribution of particles on the surface. The wavelength in these calculations is $10\text{ }\mu\text{m}$; the incident light beam is unpolarized and directed normal to the reflecting surface. The differential cross section, $d\sigma(\theta)/d\Omega$, is a function of the scattering angle, θ , which is measured with respect to the normal to the surface. The units of the differential cross section are $\text{micron}^2/\text{steradian}$. Results are calculated for two values of the particle index of refraction; $n = 1.8$, which is a transparent (nonabsorbing) material, and $n = 2.7 + 0.51j$ (where j is the imaginary unit), which is an opaque (absorptive) material.

4.1 DIFFERENTIAL CROSS SECTIONS

Figure 3a shows the differential cross sections for a small particle, diameter = $1\text{ }\mu\text{m}$. The exact cross sections are much smaller than the Mie approximation cross sections. The reason for this is easy to understand. The field strength near the conducting surface is small (because of the boundary condition), so there is no incident field amplitude available to be scattered by the particle.

Figure 3b shows cross sections for a large particle, diameter = $50\text{ }\mu\text{m}$. The most important point to note here is that the angular structure of the exact differential cross section is quite similar to that of the simple Mie theory differential cross section. The small-angle region is dominated by a large diffraction peak, which is several orders of magnitude greater than the scattering values outside of this peak. The angular width of the diffraction peak is given approximately by the formula for the first dark ring in the diffraction pattern of a circular aperture, $\theta = 1.22\lambda/d$ (radians), where λ is the wavelength and d is the particle diameter. The maximum amplitude of the diffraction peak is about a factor of 5 greater than the Mie theory prediction for the case shown in Fig 3b. In the region outside the diffraction peaks, both scattering functions have a qualitatively similar behavior although the exact solution has a more pronounced oscillatory structure.

The most pronounced difference between the exact theory and the Mie approximation differential cross-section results is evident in Figure 4. Here the scattering angles are fixed, and the differential cross sections are plotted vs the particle diameter. The exact results show a large amplitude oscillation that does not occur in the simple Mie theory results. The amplitude of the diffraction peak calculated by exact theory oscillates above and below the diffraction peak calculated by Mie theory. Figure 3b shows a case where this amplitude is near a local maximum. These oscillations in the differential cross sections could possibly have real consequences in experimental measurements of BRDF when a laser or other narrowband light source is used to illuminate the sample contaminated surface. The number density of large particles may not be sufficient to average over the effects of the oscillations. The amount of light scattered by the large particles will depend sensitively on their diameters. This could lead to large statistical fluctuations in the measured BRDF for different particle samples that appear to have the same size distribution.

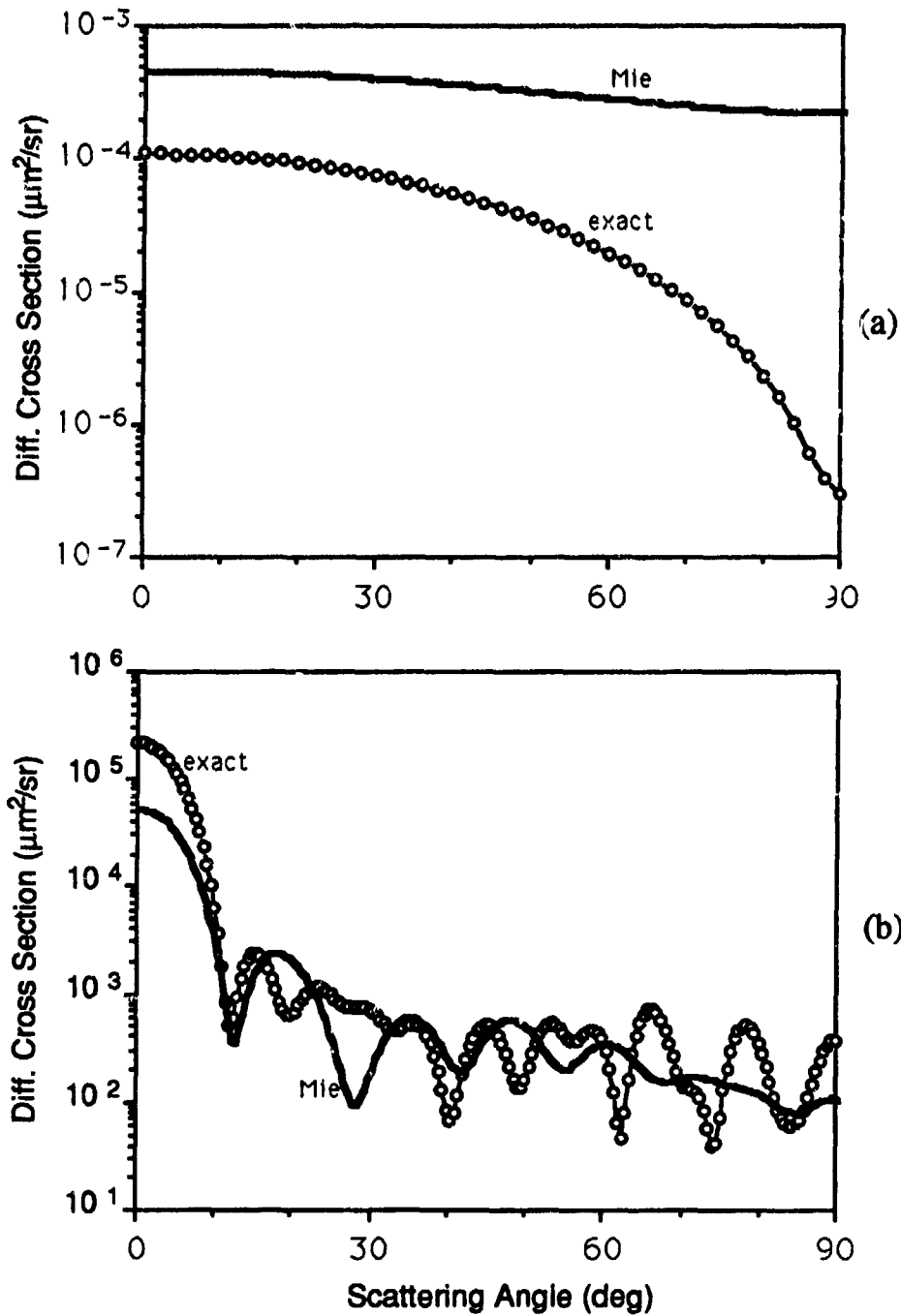


Figure 3. Differential scattering cross section for particle on mirror. Comparison of exact theory and forward-scatter Mie approximation with $n = 1.8$, $\lambda = 10\ \mu\text{m}$. (a) diameter = $1\ \mu\text{m}$; (b) diameter = $50\ \mu\text{m}$.

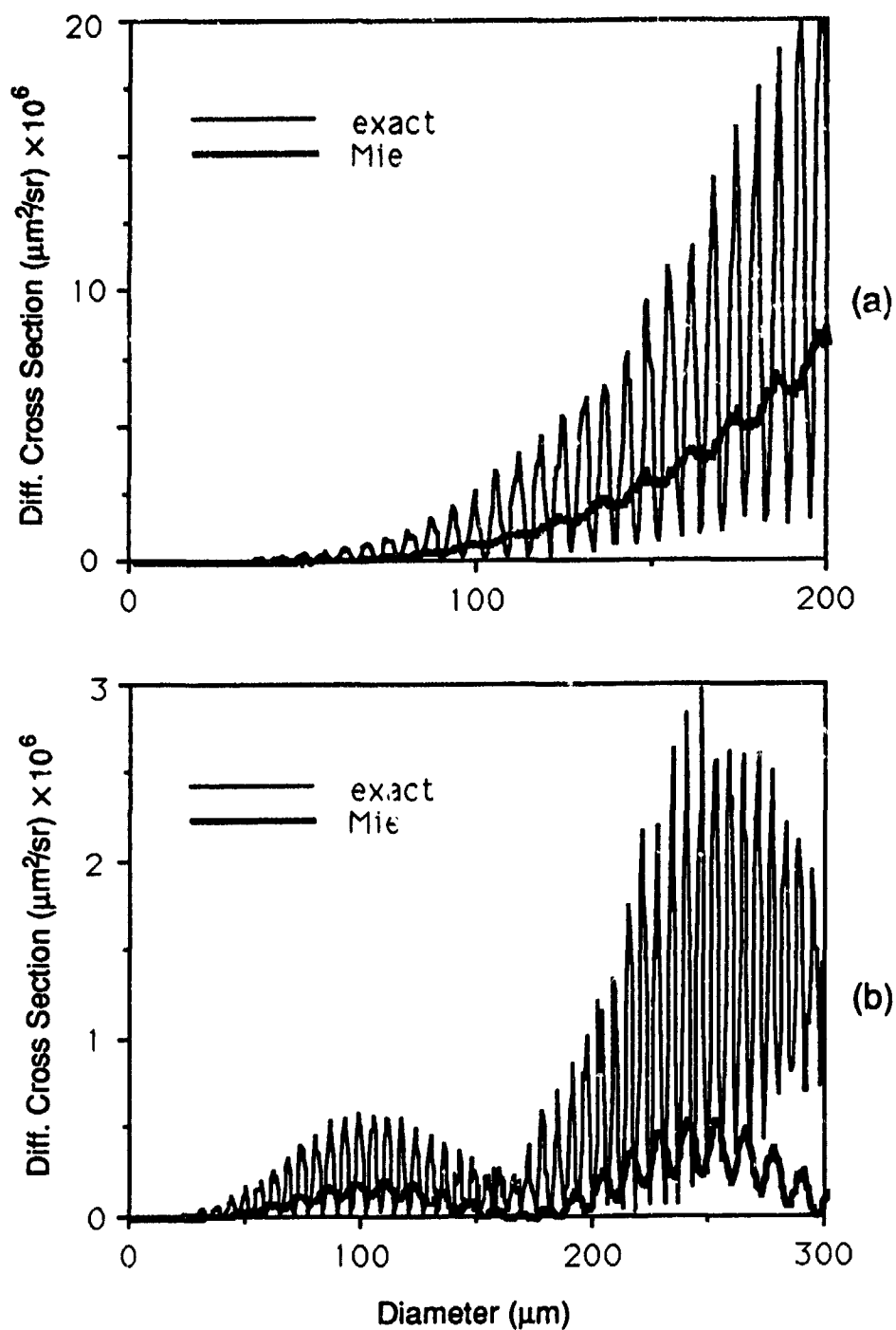


Figure 4. Differential scattering cross section vs particle diameter at fixed scattering angles, with $n = 1.8$, $\lambda = 10 \mu\text{m}$. (a) angle = 1° ; (b) angle = 4° .

Figure 5 shows similar plots for the absorptive particles. Here we see that the large oscillations in the exact solutions have been damped out at the smaller angles so there is much better agreement between exact theory and the Mie approximation. However, as Figure 5c shows, at larger scattering angles, serious differences still exist between the exact and Mie results.

4.2 BRDF

BRDF is the appropriate measure of scattered light from a distribution of particles on a surface. The distribution is characterized by the particle size density distribution function, $n(x)$. This function is defined such that $n(x)dx$ is the number of particles on the surface per unit area of surface that have diameters between the values of x and $x + dx$. The BRDF of the particle-contaminated surface is defined by the relation

$$BRDF(\theta) = \int_0^\infty n(x) \frac{d\sigma(x, \theta)}{d\Omega} dx. \quad (1)$$

This definition of BRDF does not have the $\cos(\theta)$ factor in the denominator. It is essentially the same definition used by Young¹.

The calculations were carried out using the particle size distribution that is used to define the MIL-STD-1246 surface cleanliness levels⁷. This distribution is defined by

$$\text{Log}(N) = 0.926 [\text{Log}^2(x_1) - \text{Log}^2(x)], \quad (2)$$

where N is the number of particles per ft^2 with diameter greater than x microns. The quantity x_1 is called the cleanliness level. The density function for this distribution is

$$n(x) = 1.852 \frac{\text{Log}(x)}{x} 10^{0.926 [\text{Log}^2 x_1 - \text{Log}^2 x]}. \quad (3)$$

This function is negative for $x < 1$, which is unphysical. Therefore, we arbitrarily defined $n(x) = 0$ in the range $0 \leq x < 1$. This causes no difficulty since these small particles make negligible contribution to the BRDF for $10 \mu\text{m}$ radiation.

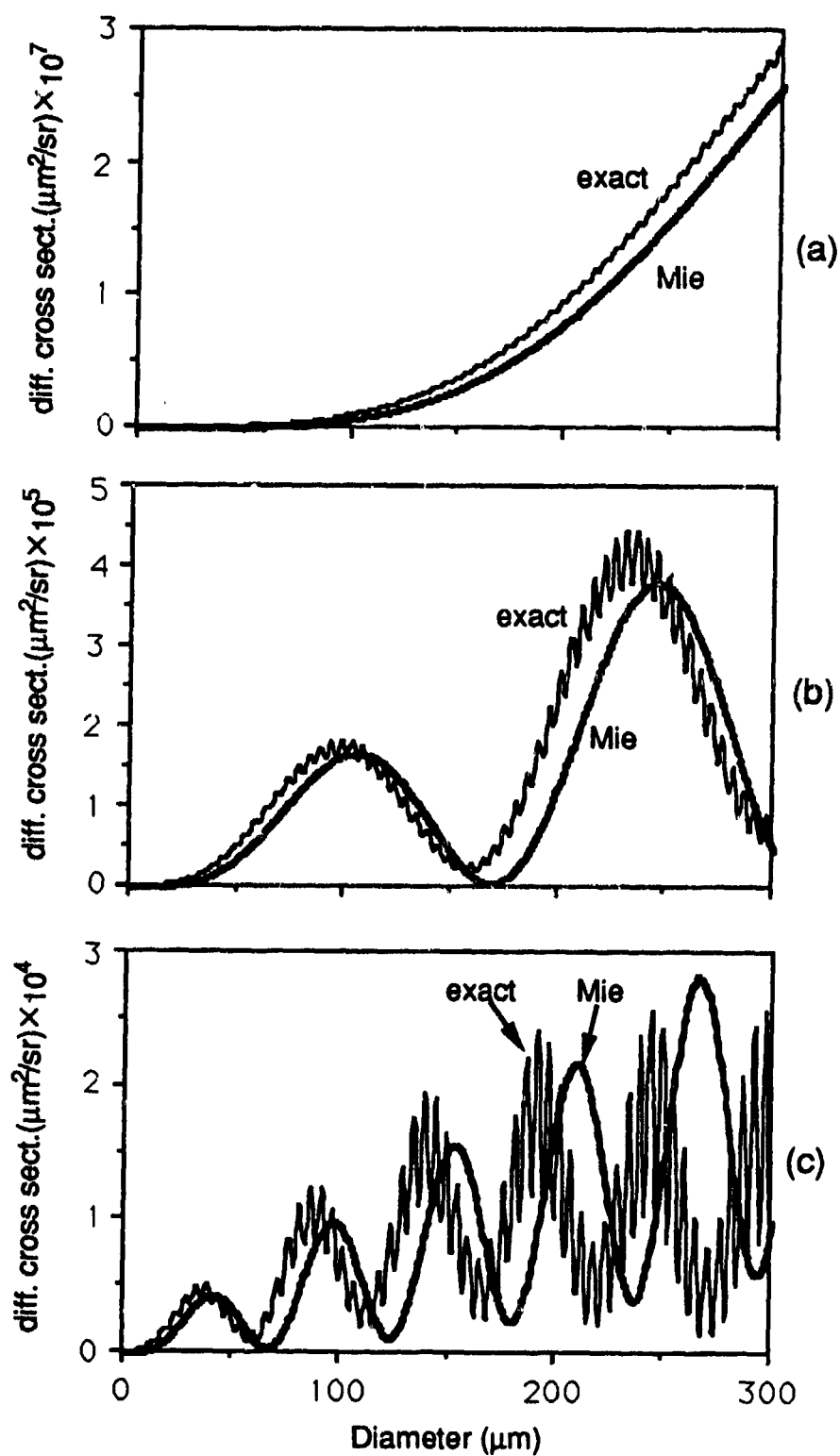


Figure 5. Differential scattering cross section vs particle diameter at fixed scattering angles, with $n = 2.7 + 0.51j$, $\lambda = 10 \mu\text{m}$. (a) angle = 1° ; (b) angle = 4° ; (c) angle = 10° .

Before actually calculating the BRDF by evaluating the integral expression in Eq. (1), it is useful to plot the integrand of the BRDF integral in Eq. (1) for selected values of θ . The integrand is a density weighted cross section given by

$$F(x, \theta) = n(x) \frac{d\sigma(x, \theta)}{d\Omega} . \quad (4)$$

Figure 6 shows the BRDF integrands for the absorptive particles for the scattering angles 1° and 10° . These curves show the relative contributions of each size particle to the total BRDF. At 1°

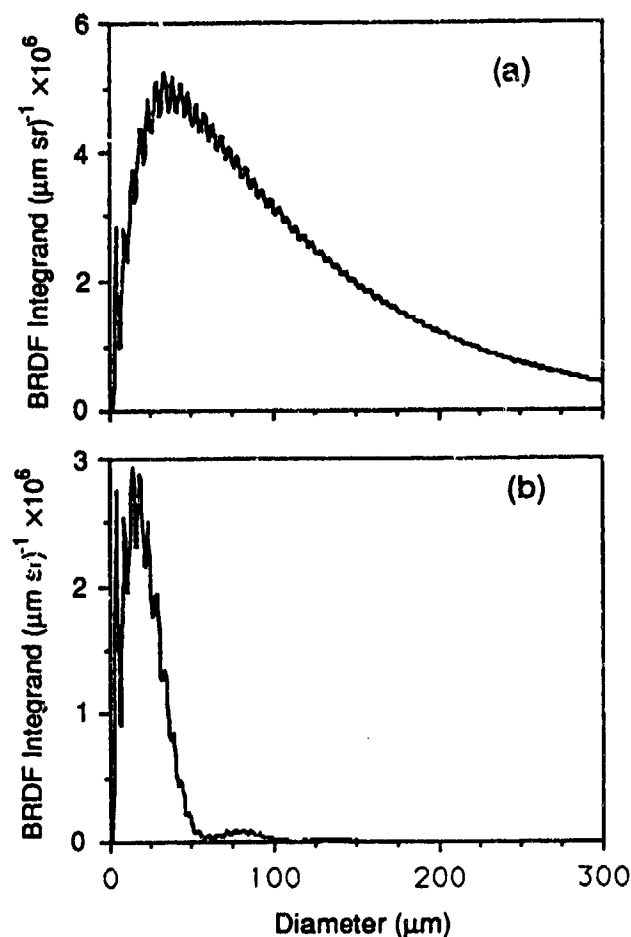


Figure 6. Density-weighted differential scattering cross section vs particle diameter at fixed scattering angles; $\lambda = 10 \mu\text{m}$, $n = 2.7 + 0.51j$; (a) angle = 1° , (b) angle = 10° .

this function has a maximum at about $50\text{ }\mu\text{m}$, and all the particles (but the very smallest) make significant contributions to the BRDF. However, at 10° , the integrand has a maximum at about $25\text{ }\mu\text{m}$, and particle sizes larger than $60\text{ }\mu\text{m}$ make very little contribution to the BRDF. The relative contribution of the various particle sizes to the BRDF is examined further by calculating the upper limits of the BRDF integral defined so that the integral evaluates to 10, 25, 50, 75, and 90 percent of the final BRDF value. These upper diameter limits are plotted as a function of the scattering angle in Figure 7. The diagram shows that at 1° , the particles with diameter greater than $100\text{ }\mu\text{m}$ contribute half of the BRDF, but at 10° these same particles contribute almost nothing.

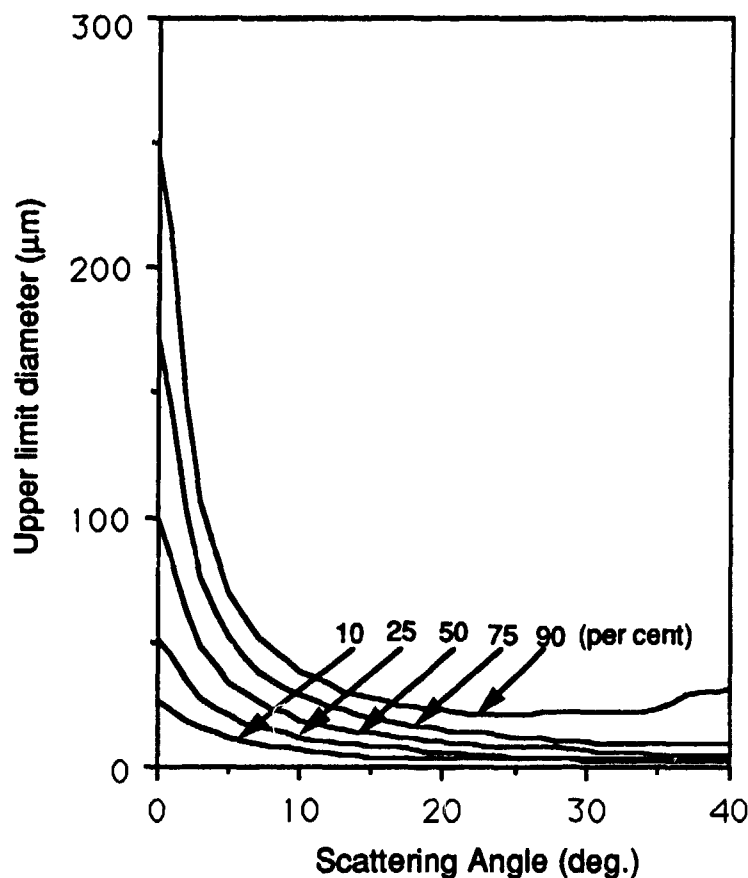


Figure 7. Upper particle diameter limit of BRDF integral that evaluates to 10, 25, 50, 75, and 90 percent of the final BRDF value.

Figure 8 compares the BRDF values calculated by exact scattering theory with the BRDF values calculated using the forward scatter Mie theory and with the exact BRDF values for hemispherical particles. The reflecting surface has an assumed cleanliness level of 300 in these calculations. In general, the exact BRDF values are larger than the Mie approximation BRDF values by about a factor of 2. In the angular range $0^\circ \leq \theta \leq 30^\circ$, Young's forward-scatter Mie approximation is seen to actually be a better approximation to the hemispherical particles than to the spherical particles.

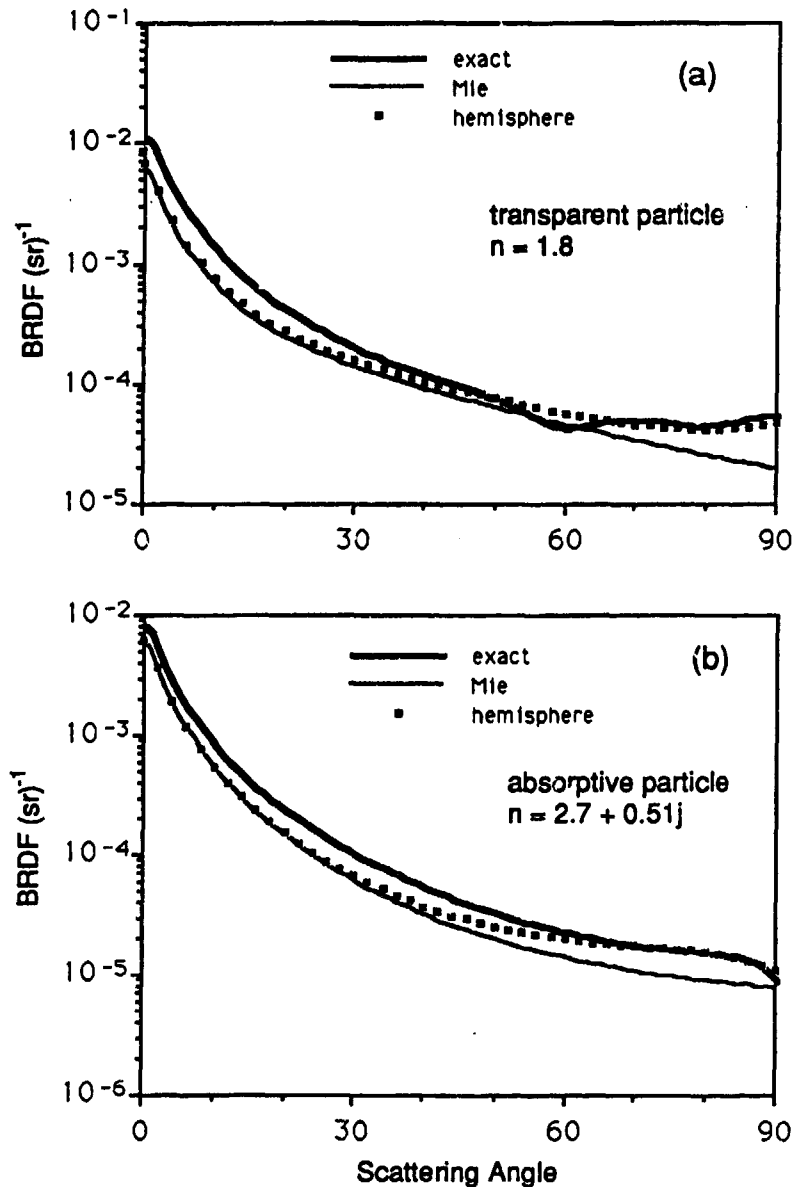


Figure 8. BRDF for cleanliness level 300 surface at $\lambda = 10 \mu\text{m}$. Comparison of exact theory for spherical particles, exact theory for hemispheres, and forward-scatter Mie theory for spherical particles. (a) $n = 1.8$, (b) $n = 2.7 + 0.51j$.

Figure 9 shows a direct comparison BRDF values for absorptive and nonabsorptive particles. As one might expect intuitively, the nonabsorptive particles produce a larger BRDF than the absorptive particles. This seems reasonable since the absorptive particles absorb part of the energy leaving less energy to be scattered.

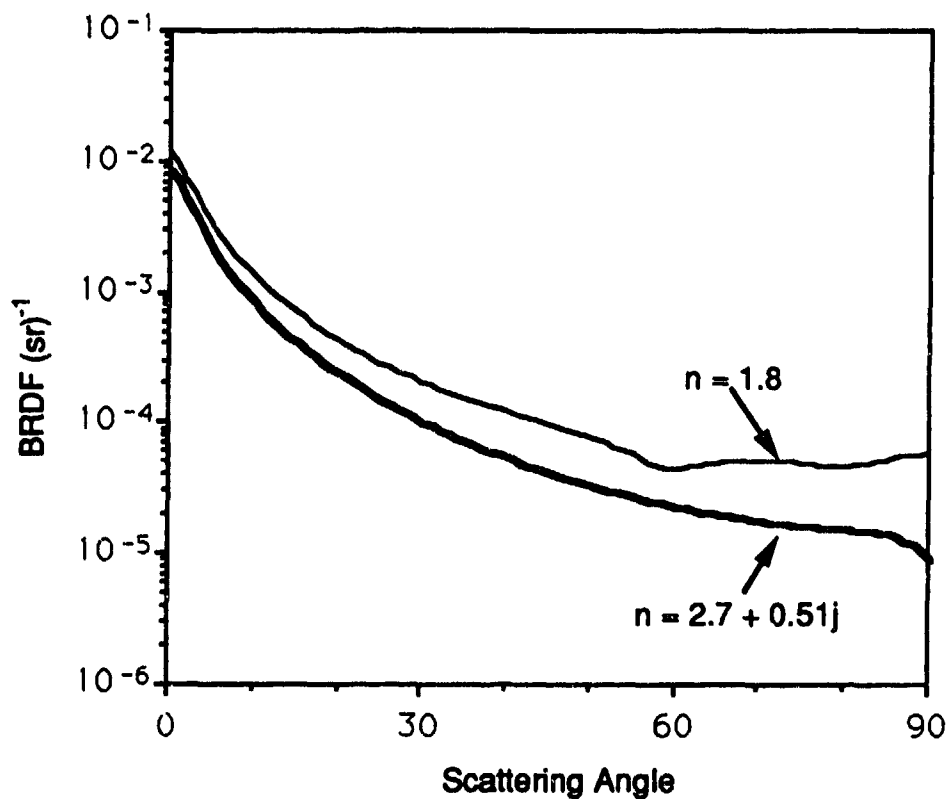


Figure 9. Comparison of BRDFs for transparent ($n = 1.8$) and absorptive ($n = 2.7 + 0.51j$) particles.

5. CONCLUDING REMARKS

An exact theory of scattering from spherical particles on a conducting plane surface was used to calculate selected differential cross section and BRDF scattering results. These exact results were compared with results obtained by Young's forward scatter Mie theory. The effect of particle shape on the BRDF was studied by comparing results for spherical particles with those for hemispherical particles. Absorbing and nonabsorbing particles were also compared.

REFERENCES

1. R. P. Young, "Low scatter mirror degradation by particle contamination," *Optical Engineering* **15**, 516-520 (1976).
2. K. B. Nahm and W. L. Wolfe, "Light scattering models for spheres on a conducting plane: comparison with experiment," *Appl. Opt.* **26**, 2995-2999 (1987).
3. D. C. Weber and E. D. Hirelman, "Light scattering signatures of individual spheres on optically smooth conducting surfaces," *Appl. Opt.* **19**, 4019-4026 (1988).
4. J. H. Bruning and Y. T. Lo, "Multiple scattering of EM waves by spheres part I - Multipole expansion and ray - optical solutions," *IEEE Trans. Antennas Propag.* **AP-19**, 378-390 (1971).
5. B. R. Johnson, "Light scattering from a spherical particle on a conducting plane: I Normal incidence," *J. Opt. Soc. Am. A* **9**, (to be published August) 1992.
6. B. R. Johnson, "Invariant imbedding T matrix approach to electromagnetic scattering," *Appl. Opt.* **27**, 4861-4873 (1988).
7. "Military standard product cleanliness levels and contamination control program", MIL-STD-1246B, Sept. 4, 1987.

INTERNAL DISTRIBUTION LIST

REPORT TITLE

Exact Calculation of Light Scattering from a Particle on a Mirror

REPORT NO.

ATR-92(8476)-1

PUBLICATION DATE

15 November 1992

SECURITY CLASSIFICATION

Unclassified

1. FOR OFF-SITE PERSONNEL, SHOW LOCATION SYMBOL,

e.g., JOHN Q. PUBLIC/VAFB

NAME (Include Initials)

MAIL CODE *

G. S. Arnold	M2/271
A. B. Christensen	M5/254
J. M. Dowling	M2/251
J. R. Hallett	M2/273
M. M. Hills	M2/271
B. R. Johnson	M2/251
H. K. Kan	M2/272
D. W. Pack	M2/251
A. T. Pritt	M2/251
C. J. Rice	M2/266
H. R. Ruge	M2/264
A. J. Schiewe	M1/002
J. J. Shaffer	M2/279
W. Von Der Ohe	M5/644

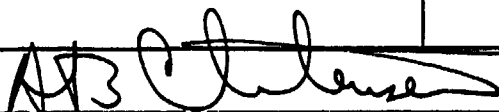
2. IF LIST IS ALTERED, INITIAL CHANGE(S) AND SHOW AFFILIATION

* FOR SECRET REPORTS SHOW BLDG AND ROOM, NOT MAIL STATION

NAME (Include Initials)

MAIL CODE *

APPROVED BY



DATE

11-16-92

IF LIST COMPRISES TWO OR MORE SHEETS, COMPLETE ABOVE BLOCK ON LAST SHEET ONLY

1

1

EXTERNAL DISTRIBUTION LIST

REPORT TITLE

Exact Calculation of Light Scattering from a Particle on a Mirror

REPORT NO.

ATR-92(8476)-1

PUBLICATION DATE

15 November 1992

SECURITY CLASSIFICATION

Unclassified

MILITARY AND GOVERNMENT OFFICES

ASSOCIATE CONTRACTORS AND OTHERS

1. SHOW FULL MAILING ADDRESS: INCLUDE ZIP CODE, MILITARY OFFICE SYMBOL, AND "ATTENTION" LINE
2. IF LIST IS ALTERED, INITIAL CHANGE(S) AND SHOW AFFILIATION

Defense Technical Information Center
Cameron Station (12 unc)
Alexandria, VA 22314
Attn: DTIC-TC

NASA Scientific and Technical Information Facility
P. O. Box 8757
Baltimore-Washington International Airport,
MD 21240
Attn: SAK/DC

Phillips Laboratory
Geophysics Directorate (OPS, LI)
Hanscom AFB, MA 01731

AEDC (ER)
Arnold AFS, TN 37389
Attn: Library

AFOSR (NC)
Bolling AFB, DC 20332

Air University Library (SE)
Maxwell AFB, AL 36112

Atmospheric Sciences Lab
SLCAS-AR-P
WSMR, NM 88002
Attn: Library

FJSRL (NA)
USAF Academy, CO 80840

Jet Propulsion Laboratory
4800 Oak Grove Drive
Pasadena, CA 91103
Attn: Library

Optical Sciences Center
University of Arizona
Tucson, AZ 85721

DISTRIBUTION LIMITATIONS MARKED ON THE COVER/TITLE PAGE ARE AUTHORIZED BY SIGNATURE BELOW

APPROVED BY _____
(AEROSPACE)

DATE _____

APPROVED BY _____
(AF OFFICE)

(NOT REQUIRED FOR ATR CATEGORY)

DATE _____

IF LIST COMPRISES TWO OR MORE SHEETS, COMPLETE ABOVE BLOCK ON LAST SHEET ONLY

SHEET 1 OF 3

EXTERNAL DISTRIBUTION LIST

REPORT TITLE

Exact Calculation of Light Scattering from a Particle on a Mirror

REPORT NO.

ATR-92(8476)-1

PUBLICATION DATE

15 November 1992

SECURITY CLASSIFICATION

Unclassified

MILITARY AND GOVERNMENT OFFICES

ASSOCIATE CONTRACTORS AND OTHERS

1. SHOW FULL MAILING ADDRESS: INCLUDE ZIP CODE, MILITARY OFFICE SYMBOL, AND "ATTENTION" LINE
2. IF LIST IS ALTERED, INITIAL CHANGE(S) AND SHOW AFFILIATION

U. S. Department of Commerce
Environmental Sciences Services Administration
Boulder Laboratories
Boulder, CO 80302
Attn: Library

NASA
Marshall Space Flight Center
Huntsville, AL 35812
Attn: Library

NASA
Lewis Research Center
21000 Brookpark Road
Cleveland, OH 44135
Attn: Library

National Institute of Standards and Technology
(NIST)
Bldg. 101, Rm E 106
Gaithersburg, MD 20899
Attn: Library

ONR-Monterey
P.O. Box 8747
Naval Postgraduate School
Monterey, CA 93943
Attn: Library

NASA
Ames Research Center
Moffett Field, CA 94035
Attn: Library

DISTRIBUTION LIMITATIONS MARKED ON THE COVER/TITLE PAGE ARE AUTHORIZED BY SIGNATURE BELOW

APPROVED BY _____
(AEROSPACE)

DATE _____

APPROVED BY _____
(AF OFFICE)

(NOT REQUIRED FOR ATR CATEGORY)

DATE _____

IF LIST COMPRISES TWO OR MORE SHEETS, COMPLETE ABOVE BLOCK ON LAST SHEET ONLY

SHEET 2 OF 3

EXTERNAL DISTRIBUTION LIST

REPORT TITLE

Exact Calculation of Light Scattering from a Particle on a Mirror

REPORT NO.

ATR-92(8476)-1

PUBLICATION DATE

15 November 1992

SECURITY CLASSIFICATION

Unclassified

MILITARY AND GOVERNMENT OFFICES

ASSOCIATE CONTRACTORS AND OTHERS

1. SHOW FULL MAILING ADDRESS: INCLUDE ZIP CODE, MILITARY OFFICE SYMBOL, AND "ATTENTION" LINE
2. IF LIST IS ALTERED, INITIAL CHANGE(S) AND SHOW AFFILIATION

NASA
Langley Research Center
Langley Field, Hampton, VA 23665-5225
Attn: Library

NASA
Johnson Space Center
Houston, TX 77058
Attn: Library

NASA
Goddard Space Flight Center
Greenbelt, MD 20771
Attn: Library

Naval Research Laboratory
Washington, DC 20025
Attn: Library

DISTRIBUTION LIMITATIONS MARKED ON THE COVER/TITLE PAGE ARE AUTHORIZED BY SIGNATURE BELOW

APPROVED BY
(AEROSPACE)

AB [Signature]

DATE 11-16-92

APPROVED BY
(AF OFFICE)

(NOT REQUIRED FOR ATR CATEGORY)

DATE

IF LIST COMPRISES TWO OR MORE SHEETS, COMPLETE ABOVE BLOCK ON LAST SHEET ONLY